Delft University of Technology

Localization of cosmic gamma-ray bursts in interplanetary space with MGNS/BepiColombo and HEND/Mars Odyssey experiments

Kozyrev, A. S.; Benkhoff, J.; Litvak, M. L.; Golovin, D. V.; Quarati, F.; Sanin, A. B.

Important note
To cite this publication, please use the final published version (if applicable).
Please check the document version above.

Localization of cosmic gamma-ray bursts in interplanetary space with MGNS/BepiColombo and HEND/Mars Odyssey experiments

A.S. Kozyrev [a,*], J. Benkhoff [b], M.L. Litvak [a], D.V. Golovin [a], F. Quarati [c,d], A.B. Sanin [a]

[a] *Institute for Space Research, Profsojuznaja 84/32, 117997, Moscow, Russian Federation*
[b] *European Space Agency, ESTEC, Keplerlaan 1, 2201 AZ Noordwijk, the Netherlands*
[c] *Gonitec BV, J. Bildersstraat 43, 2596 EE Den Haag, the Netherlands*
[d] *Delft University of Technology, Faculty of Applied Sciences, Department of Radiation Science and Technology, Section Luminescence Materials, Mekelweg 15, Delft, 2629 JB, the Netherlands*

ABSTRACT

This paper describes the methods and results for the localization by triangulation of cosmic gamma-ray bursts (GRBs) independently observed by two space experiments: the Mercury Gamma-ray and Neutron Spectrometer (MGNS) and the High Energy Neutron Detector (HEND). MGNS is onboard the MPO/BepiColombo mission and on a stage of cruise to Mercury whereas HEND is onboard Mars Odyssey mission and in orbit around Mars. An analysis is performed of the accuracy of localization of the GRBs jointly observed by the two instruments at interplanetary distances by comparing their light curves. Notable achievements and scientific opportunities are described also in light of the recent inclusion of MGNS within the program of interplanetary network for gamma-ray burst localization (IPN).

1. Introduction

Localization of cosmic gamma-ray bursts (GRBs) gives the opportunity to perform observations to search the GRB counterpart in the optical and radio energy ranges. GRB afterglow observations are crucially important to foster knowledge and understanding of the nature of GRB. At present, various scientific instruments onboard dedicated space missions, such as Swift (NASA) (Gehrels et al., 2004), FERMI (NASA) (Paciesas et al., 2012), GECAM (CNSA) (Chen et al., 2021), INTEGRAL (ESA) (Winkler et al., 2003) and AGILE (ASI) (Tavani et al., 2008) can independently observe and localize GRBs. In addition, GRBs are observed using instruments onboard the miniaturized satellite CubeSat (e.g. GRBAlpha and VZLUSAT2). On the other hand, the localization of GRBs can also be performed by triangulation technique using the data from two or more instruments, potentially achieving a more precise localization than the one performed by a particular space science instrument alone (Hurley et al., 2013). The principle of such localization is shown in Fig. 1. In this case, the localization accuracy is inversely proportional to the distance between the instruments that jointly detect a certain GRB. The Interplanetary Network (IPN) operates such localization (Hurley et al., 2013) and includes a group of spacecrafts in the near-to-Earth orbit (i.e. Konus-Wind, INTEGRAL, AGILE and Swift) and the High Energy Neutron

Detector (HEND) instrument onboard Mars Odyssey, orbiting Mars.

The prompt exchange of information on the localization of the gamma-ray burst is also critical for the study of the afterglow. The afterglow could last for a few days (Gendre et al., 2009 and Zhang et al., 2006). Our preliminary experience shows that typical time required for the high accuracy localization of GRB using HEND and MGNS data and public release of this information is about 1–2 days after receiving the data. The Gamma-ray Coordinates Network (GCN) is used for prompt exchange, which distributes information about the events detected by various experimental setups and spacecraft's (https://gcn.gsfc.nasa.gov/). The IPN also uses the GCN system to exchange information about detected and localized GRB. Presently, we are working on a smart algorithm to convert the above into an automatic and time effective procedure.

After the launch of BepiColombo on October 20, 2018, its payload experiment named Mercury Gamma-ray and Neutron Spectrometer (MGNS) provides another interplanetary location for observation of GRBs, potentially increasing IPN's localization capability and accuracy. In fact, since October 20, 2021, MGNS became part of IPN (Hurley 2021). As further detailed in Section 2, MGNS and HEND instruments are developed to provide GRB detection capability in addition to their primary scientific tasks. In this paper we present the methodology
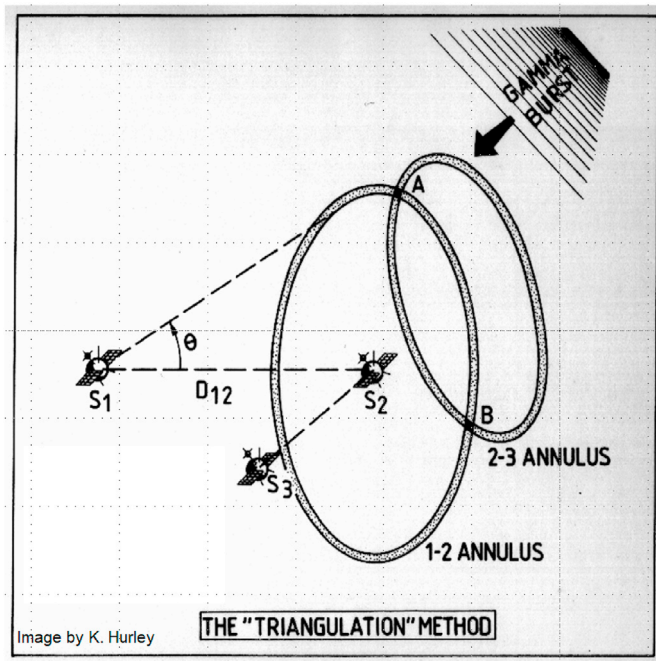

Fig. 1. The triangulation technique from Hurley et al. (2013).

developed for localizing GRB sources by combining data from the MGNS and HEND instruments and provide case studies of its benefits.

The paper is organised to provide in Section 2 a focused description of MGNS and HEND whereas Section 3 reports the methodology of localization by triangulation applicable to MGNS and HEND. Section 4 provides a review of confirmed GRB events so far jointly observed by MGNS and HEND. Section 5 summarises present achievements.

2. MGNS and HEND instruments

The HEND instrument (see Fig. 2) is developed for monitoring neutron and gamma-ray fluxes from the surface of Mars (Mitrofanov et al., 2003). It is one of the instruments of the Gamma-Ray Spectrometer Suite onboard Mars Odyssey mission (Boynton et al., 2003) aimed to the study of the elemental composition of the Martian surface by gamma-ray and neutron spectroscopy methods. One of the additional scientific tasks of the HEND is to register GRBs. HEND instrument includes the Sensor of High Energy Neutron detector (SHEN), comprising of a stilbene scintillator crystal surrounded on three sides (except for the direction toward the Mars surface) by an anticoincidence CsI inorganic scintillator crystal.

In addition to the neutron signal, the output of the SHEN detector includes two gamma-ray signals: one from the stilbene (400 keV - 3 MeV) and the other from the CsI (60 keV–1.3 MeV). These two gamma-ray signals are continuously measured with a resolution of 1 s and 0.25 s, respectively. HEND instrument provides an omnidirectional gamma ray sensitivity and the effective area of its CsI setector is about 10 cm^2 (Livshits et al., 2017). Naturally, the most appropriate data for high precision localization of gamma-ray bursts are that with 0.25 s time resolution from the CsI. As general practice, data transfer from the HEND instrument to ground takes place on a daily cycle. In operation since 2001 and part of IPN since 2002, HEND provides the IPN an observation point at interplanetary distance from Earth, ranging from 200 to 1300 light-seconds.

The MGNS onboard BepiColombo's Mercury Planetary Orbiter (MPO) is developed to measure the gamma-ray and neutron fluxes from Mercury's surface for the study of its elemental composition (Mitrofanov at al, 2010 and 2021). The design of MGNS is partially adapted from that of HEND in regard to the neutron detector, operating logic and electronics, see also Fig. 2. Moreover, MGNS includes a gamma-ray spectrometer (GRS) based on a $3'' \times 3''$, high energy resolution, CeBr$_3$ inorganic scintillator crystal (Kozyrev et al., 2016, Kozyrev et al., 2016). Its main purpose is the detection of nuclear gamma-ray lines associated with elements in the subsurface layers of Mercury. As an additional scientific task, the GRS can detect GRBs. The GRS generates two types of data: gamma-ray energy spectra and integral count rates. The energy spectra (of 4071 channels) can be measured with accumulation time of 20–2400 s and in the energy range from 250 keV up to 10 MeV. As HEND, MGNS instrument is an omnidirectional gamma-spectrometer. Count rates are measured in two energy ranges: from 250 to 440 keV; and from 650 to 8000 keV; and with accumulation time from 0.125 up to 8 s. Obviously, the duration of data accumulation determines the temporal resolution of the data. The time resolution in the current cruise phase can be remotely controlled by specific commands, following considerations that include also practical aspects as, e.g., the availability of memory buffers for data storage and the capabilities of data transmission to Earth. As optimum compromise, it is envisaged to use 20 s for spectral data and 1–5 s for integral count rates. It is expected that measurements of the integrated count rate in the energy range from 250 to 440 keV with a time resolution of 1–5 s can be used to localize gamma-ray bursts with high accuracy by the triangulation technique.

Launched in October 2018, BepiColombo (Benkhoff et al., 2021) will continue until December 2025 its cruise phase on a near-Mercurian elliptical Sun orbit hence with a varying interplanetary distance from Mars. After being captured by Mercury and inserted into its final polar orbit (480 × 1500 km), BepiColombo will start the planet's exploration phase in April 2026. This phase (1 year nominal and 1 year extension) will continue until May 2028. It is expected that during the exploration

Fig. 2. MGNS instrument (left) and HEND instrument (right) integrated into the ESA BepiColombo Mercury Planetary Orbiter and NASA Mars Odyssey flight spacecraft, respectively.

phase, MGNS data will be transmitted to the ground with a frequency of once every 1–3 days, except for a few periods when there will be no data transmission because of mission operation constraints. During the cruise phase, data are transmitted with a frequency that changes from several times per day up to once a week, depending on the capability of the spacecraft to transmit data and on mission operation constraints.

Both MGNS and HEND instruments were developed and manufactured at the Space Research Institute of the Russian Academy of Sciences and are a Russian-made and Russian-funded contribution by the Russian Federal Space Agency (ROSCOSMOS) to the BepiColombo and Mars Odyssey missions, respectively.

3. Analysis of the MGNS and HEND light curves and localization

Using the formulation by Hurley et al. (2013), a GRB jointly observed by MGNS and HEND with a time delay ΔT can be localized as a ring on the astronomical sphere with a corner angle θ with respect to the vector between the two spacecrafts (see Fig. 1). The angle θ is defined as:

$$cos(\theta) = \frac{C\Delta T}{D_{12}} \qquad (1)$$

where D_{12} is the distance between the BepiColombo and Mars Odyssey spacecrafts, C is the speed of light, ΔT is delay time of gamma-ray burst detection by HEND and MGNS instruments. The annulus width $\delta\theta$ is determined by the accuracy in timing the detection of a single GRB by the two gamma-ray detectors $\delta(\Delta T)$ and by the accuracy in determining their relative position in space. It is important that the accuracy of GRB localization increases with increasing distance D_{12} and with increasing timing accuracy, i.e. minimising $\delta(\Delta T)$. The systematic uncertainty in determining the relative position of the Mars Odyssey and BepiColombo spacecraft is determined for each spacecraft and taken into account in the corresponding kernels that are included in the SPICE system (Acton 1996 and Acton et al., 2017). But in any case it is much less than statistical uncertainty derived from the correlation between MGNS and HEND light curves.

The timing accuracy is strongly related to the duration of the instrument's data acquisition interval, which in turn is determined by the need to accumulate a statistically significant number of counts during each interval. The limited sensitivity of the detector, determined by its geometric dimensions and the type of scintillation crystal used, does not allow one to choose an arbitrarily small data accumulation interval and, thus, increase the timing accuracy. Therefore, the main way to increase the accuracy of localization of gamma-ray bursts by the triangulation technique is to increase the distance between the detectors to interplanetary ranges.

As described in Section 2, for high-precision localization of GRBs, the HEND data with time resolution of 0.25 s from the CsI scintillator crystal are used. MGNS data present instead a variable time resolution typically from 1 up to 5 s, constrained by the mode of operation of the instrument following chiefly mission control requirements and recommendations. Fig. 3 presents the GRB190530A as observed by both MGNS and HEND in terms of count rate variations over time also known as "light curves".

With reference to Fig. 4, in order to evaluate the delay time ΔT, a procedure was established in which the light curve of HEND is aligned on top of that of MGNS by applying Pearson's chi-squared statistical test. This approach is commonly used also within the IPN. Since the two instruments operate with different time resolutions, the light curves must be converted to a uniform time resolution in order to be aligned. Moreover, it is convenient to operate the alignment in small steps so to enhance the precision of the evaluation. Hence, we first proceed by oversampling HEND data by dividing each of its 0.25 s bins into 5 subbins of 0.05 s each. This allowed to operate the light curve alignment in steps interspaced by 0.05 s time-shifts. At each step, HEND data were, first, again rebinned from 0.05 s to the time resolution of the MGNS, which ranged from 1 s to 5 s. Such a rebinning implies that some of HEND
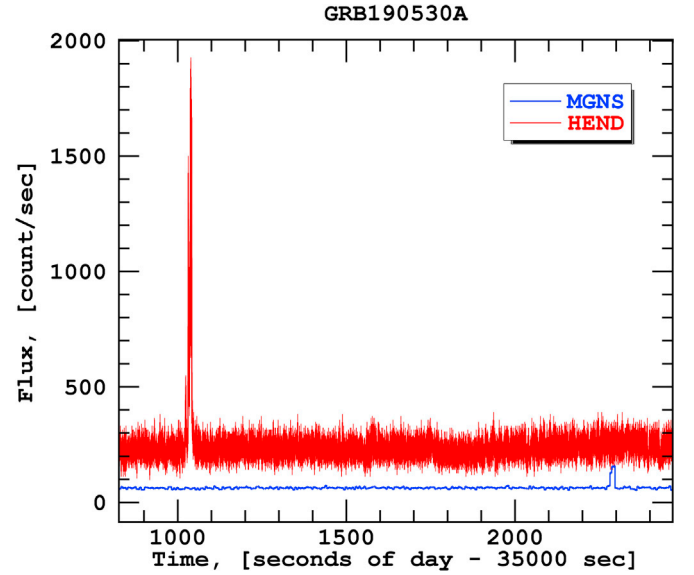

Fig. 3. MGNS (blue line) and HEND (red line) light curves for GRB190530A with time resolution of 5 s and 0.25 s, respectively.
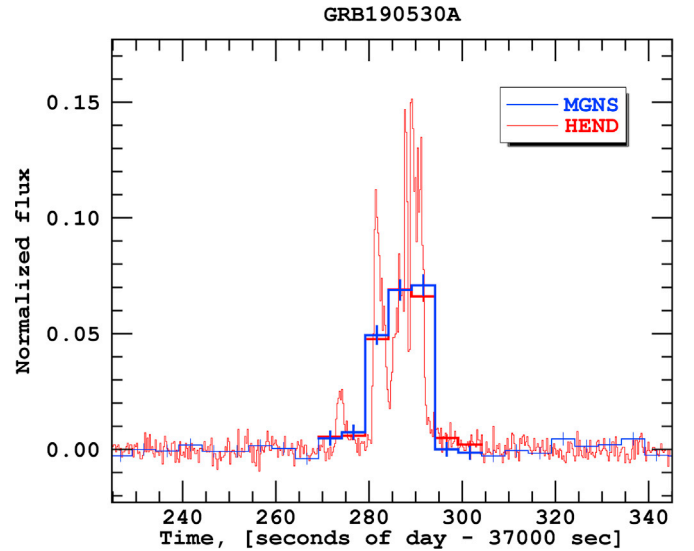

Fig. 4. MGNS (blue line) and HEND (red line) light curves with background subtracted and flux normalized are aligned for the best fit for the burst of GRB190530A in MGNS detection time. The MGNS and HEND light curves are presented with a time resolution of 5 s and 0.25 s, respectively. The thick red and blue lines show the bins that are taking part in the fitting. The statistical uncertainty at each bin is shown by vertical line. The HEND data have been oversampled within the 5 s of MGNS time resolution.

original 0.25 s bins, are split partially in one bin and partially in the next one. In case of the most common MGNS binning of 1 s, up to 5 original HEND bins of 0.25 s are used with at least three remaining unsplit. In addition, prior to the fitting, both light curves were background subtracted and normalized to a unit area. Equal interval of times, and hence number of bins, were used at each step of the whole alignment process.

The function χ^2 was calculated using the formula:

$$\chi^2(\Delta \boldsymbol{T}) = \sum_{i=1}^{n} \frac{\left(C_i^M - C_i^H(\Delta T)\right)^2}{\sigma_i^2} \qquad (2)$$

where n is the number of bins selected for analysis for both instruments; C_i^M and $C_i^H(\Delta T)$ – the normalized counting rates in bin i for MGNS and

HEND data, respectively; σ_i^2 – statistical uncertainty of values for C_i^M and $C_i^H(\Delta T)$. As mentioned, the light curve from HEND was shifted relative to that of MGNS by steps of 0.05 s and then converted to the time resolution of MGNS (ranging from 1 s to 5 s). For each step, a value of the χ^2 was calculated. Fig. 4 shows the result of the described alignment procedure for the GRB190530A burst, in terms of χ^2 vs. time shift and the sought delay time, ΔT, corresponds to the χ^2 minimum. The delay time uncertainty $\delta(\Delta T)$ was calculated based on the minimization of the χ^2 function statistics for one-parameter function and at the 68% and 99% confidence levels (significance of 1 σ and 3 σ, respectively). See the example of χ^2 function in Fig. 5. The detailed procedure followed for calculate $\delta(\Delta T)$ is available from Lampton et al. (1976).

Based on the calculated delay ΔT, considering the associated uncertainty $\delta(\Delta T)$, the corresponding annulus of width $\delta\theta$ can then be evaluated using equation (1). The coordinates of the GRB source in terms of annuli with a probability of 68% and 99% (significance levels 1 σ and 3 σ respectively) are then extracted.

In order to validate the above procedure, the GRB localizations carried out with MGNS and HEND data were compared with that obtained independently by other space instruments, as well as with that obtained by the IPN network. Results indicate that MGNS-HEND data can significantly improve GRB localization as shown in Fig. 6 for the example of the GRB200219C with detected and confirmed optical transient. This figure shows how the MGNG and HEND data provide a significant reduction of the area of the sky corresponding to the probable location of the GRB source obtained from the FERMI data. Moreover, the associated optical transient (Xu et al., 2020 (GCN27161) and Reva et al., 2020 (GCN27162)) and the associated radio transient (Cunningham et al., 2020, (GCN27298)), are both located within the localization region of MGNS-HEND.

In our analysis the time delay ΔT determination was implemented on the well etablished Pearson's criterion. Within the IPN, this approach was being used for many years in data analysis for GRB localization when only HEND data were available (see, e.g. Pal'shin 2013). Not to introduce additional systematic uncertainties, this method was also applied for the joint analysis of HEND and MGNS data. It was successfully tested on GRB's which have a very good localization, even without HEND and MGNS data. Now, there are alternative methods to estimate best fit value of time delay ΔT. One of them is based on cross correlation analysis
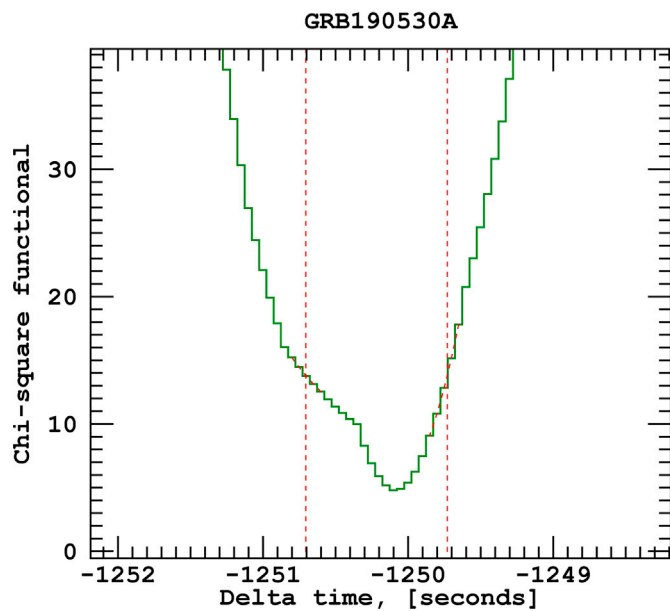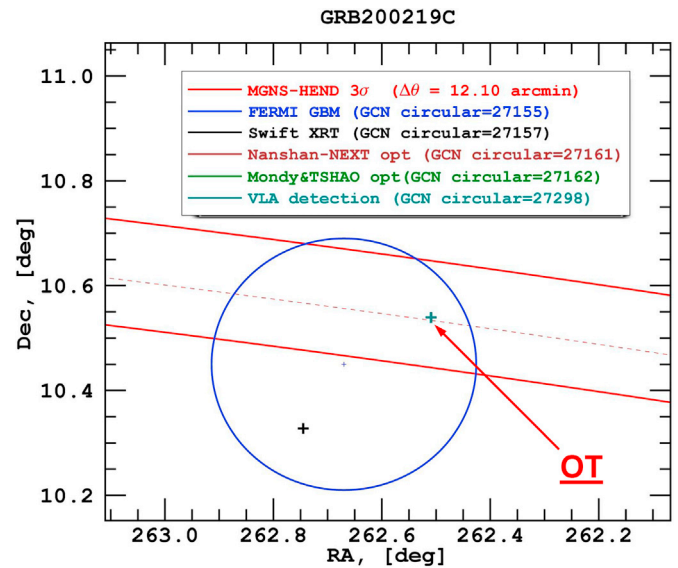

Fig. 6. MGNS-HEND triangulation annulus for the bursts GRB200219C from Group 1 (see Section 4). The red arrow indicates the crosses marks of optical and X-ray counterpart associated with GRB200219C source (GSN circular 27161, 27162 and 27298).

(Sanna et al., 2020). In the next update of HEND-MGNS GRB's localization procedure we plan to implement different techniques and to test how they could improve localization.

4. Results

Between April 2019 and November 2021, HEND and MGNS detected 130 and 43 confirmed GRBs, respectively. These GRBs were also detected by other experiments and the findings are published in the Gamma-Ray Burst Coordinates Network Circulars (GCN, see https://gcn.gsfc.nasa.gov/gcn3_archive.html). The relatively low rate of GRB detected by MGNS arises mainly from the GRBs detection limitation listed below:

- *Limitation 1* is related to a relatively high energy threshold for gamma-photon. Prime purpose of MGNS is that of detecting high energy gamma ray from of Mercury's sub surface rather than GRBs. Thus, for MGNS, the lower energy threshold for gamma-ray spectroscopy is about 300 keV, which significantly prevents the detection of all those GRBs with a main emission below that threshold. These GRBs correspond to a significant part of all GRBs triggered by the Fermi/GBM and SWIFT/BAT in the energy range 50–300 keV.
- *Limitation 2* – the temporal resolution during the registration of gamma-ray bursts by MGNS instrument varies from 1 to 8 s. This limitation deprives MGNS instrument of the possibility of detecting a group of short gamma-ray bursts with a duration T_{90} of less than 1 s (Kouveliotou et al., 1993).
- *Limitation 3* – the total number of GRBs detected by MGNS is also affected by the actual operation time, about 74%. In fact, MGNS is typically switched off at least during solar conjunction and trajectory and orientation corrections and other mission operation manoeuvres.
- *Limitation 4* – since HEND operates in the orbit around Mars, a part of the sky is blocked by the planet, which prevents registration of GRBs occurring behind the planet.

Thus, considering the described *Limitations 1–4*, the number of 24 GRB jointly detected by MGNS and HEND is consistent with expectations. The list of these 24 GRB is presented in Table 1. For these GRB, we applied the light curve fitting procedure as described in Section 3 and estimated the localization of the source on the celestial sphere in the form of an annulus. Localization data at the 3 sigma level of uncertainty are

Fig. 5. Example of Chi-square function graph dependence of light curve comparison. Vertical red lines show the 3σ confidence interval of best cross-correlation value of time delay ΔT.

Table 1
List of localized gamma-ray bursts by the light curves from MGNS and HEND experiments with mention of available localization data and optical observations taken from the GCN Circulars by other experiments.

#	GRB name	GRB data and time	Experiments that provided localization areas for GRB sources in GCN circulars.						Optical observations of GRB sources.			Group
			FERMI	BALROG	IPN	SWIFT BAT	AGILE GRID	GECAM	Opt. source conf.[a]	No opt. source detected[b]	No opt. source measur.[c]	
1	GRB 190501A	01.05.2019 05:23:23	no	no	YES	no	YES	not operated	-	+	-	Group 2
2	GRB 190530A	30.05.2019 10:19:08	YES	YES	no	no	YES	not operated	+	-	-	Group 1
3	GRB 191202A	02.12.2019 20:48:51	YES	YES	no	no	no	not operated	-	-	+	Group 2
4	GRB 200125B	25.01.2020 20:43:31	YES	YES	YES	no	no	not operated	-	+	-	Group 2
5	GRB 200219C	19.02.2020 23:57:10	YES	YES	no	no	no	not operated	+	-	-	Group 1
6	GRB 200313A	13.03.2020 01:41:36	YES	YES	YES	no	no	not operated	-	-	+	Group 2
7	GRB 200326B	26.03.2020 21:13:52	no	no	no	no	no	not operated	-	-	+	Group 4
8	GRB 200415A	15.04.2020 08:48:05	YES	YES	YES	no	no	not operated	+	-	-	Group 1
9	Not in GCN	18.05.2020 17:25:01	no	no	no	no	no	not operated	-	-	+	Group 4
10	GRB 200716A	16.07.2020 01:26:37	YES	YES	YES	no	no	not operated	-	+	-	Group 2
11	GRB 200716C	16.07.2020 22:57:41	YES	YES	no	YES	no	not operated	+	-	-	Group 1
12	GRB 200826B	26.08.2020 22:09:42	YES	YES	YES	no	no	not operated	-	+	-	Group 2
13	GRB 200829A	29.08.2020 13:59:34	YES	no	no	no	no	not operated	+	-	-	Group 1
14	GRB 200903E	03.09.2020 02:34:27	no	no	YES	no	no	not operated	-	-	+	Group 2
15	GRB 201103B	03.11.2020 18:06:45	no	no	YES	no	no	not operated	+	-	-	Group 1
16	GRB 201218A	18.12.2020 04:14:15	YES	YES	YES	no	no	no	-	+	-	Group 2
17	GRB 210112A	12.01.2021 01:37:03	no	no	no	YES	no	no	+	-	-	Group 1
18	GRB 210121A	21.01.2021 18:41:48	no	no	YES	no	no	YES	-	-	+	Group 2
19	GRB 210619B	19.06.2021 23:59:25	no	no	no	YES	no	YES	+	-	-	Group 1
20	GRB 210812A	12.08.2021 16:47:01	YES	YES	no	no	no	no	-	+	-	Group 3
21	GRB 210927B	27.09.2021 23:54:45	YES	no	no	no	no	YES	-	-	+	Group 3
22	GRB 211019A	19.10.2021 05:59:31	YES	YES	YES	no	no	no	-	+	-	Group 2
23	GRB 211022A	22.10.2021 00:47:28	no	no	YES	no	no	YES	-	-	+	Group 2
24	GRB 211120A	20.11.2021 23:05:21	no	no	YES	no	YES	YES	-	-	+	Group 3

[a] Optical transient was detected and its position is confirmed by the source localization area obtained from the MGNS-HEND data.
[b] Optical transient was searched without being detected.
[c] No optical transient search was performed.

presented in Table 2. In Table 1, the independent localization of the actual GRBs by other experiments (FERMI/BAT, BALROG, SWIFT/BAT, AGILE/GRID, GECAM or IPN program) is reported along with observation of optical transient (OT). Of particular relevance in the data in Table 1, it is that, among the group of analyzed GRBs, no events were localized by all space instruments at once. Reasons for this include: one or more instruments can be in planet-blocked regions; the energy range or temporal resolution did not allow detection; one or more instruments were simply non-operating when the GRB occurred. For the same reasons, also the search by the IPN program does not always succeed in localizing a particular GRB (Hurley et al., 2016). In this scenario, the inclusion of the MGNS-HEND pair as a new kind of accurate localization provides crucial additional opportunity in the search of transients associated to GRBs.

After analysis, the 24 gamma-ray bursts presented in Table 1 were combined into four groups. The definition of each group is given in Table 3.

Group 1 includes 8 GRBs for which ground-based optical observations have been performed and an optical transient has been detected and identified with the source of the corresponding GRB. The 8 GRBs of *Group 1* were also used to verify the localization method of Section 3. The ground-based optical observations showed that all GRB sources of *Group 1* are located within the MGNS-HEND localization area on the 3σ significance level. An example of the localization of a gamma-ray burst GRB200219C from *Group 1* is shown in Fig. 6.

Group 2 includes 11 GRBs for which localization error box have been calculated and published in GCN circulars by the instrument teams of FERMI, BALROG, AGILE and GECAM or by IPN project teams (see

Table 2
List of GRB triangulation annuli by MGNS-HEND data at the 3 sigma uncertainty level.

#	GRB name	GRB data and time	MGNS-HEND 3 sigma annuli					
			R.A. (J2000), [deg]	Dec. (J2000), [deg]	R, [deg]	+dR, [deg]	-dR, [deg]	ΔR, [ang. min.]
1	GRB 190501A	01.05.2019 05:23:23	264.532	−24.488	111.921	+0.067	−0.184	+15.031
2	GRB 190530A	30.05.2019 10:19:08	282.996	−24.235	161.160	+0.078	−0.053	+7.857
3	GRB 191202A	02.12.2019 20:48:51	28.319	11.172	130.319	+0.120	−0.059	+10.764
4	GRB 200125B	25.01.2020 20:43:31	67.108	22.094	56.538	+0.009	−0.012	+1.269
5	GRB 200219C	19.02.2020 23:57:10	87.721	24.061	145.033	+0.089	−0.112	+12.097
6	GRB 200313A	13.03.2020 01:41:36	106.314	23.487	30.518	+0.250	−0.244	+29.638
7	GRB 200326B	26.03.2020 21:13:52	117.871	22.018	112.043	+0.182	−0.116	+17.884
8	GRB 200415A	15.04.2020 08:48:05	133.351	18.699	125.697	+0.093	−0.017	+6.568
9	Not in GCN	18.05.2020 17:25:01	154.651	11.728	119.103	+0.061	−0.080	+8.440
10	GRB 200716A	16.07.2020 01:26:37	176.552	3.117	41.764	+0.092	−0.086	+10.667
11	GRB 200716C	16.07.2020 22:57:41	176.574	3.127	32.260	+0.107	−0.102	+12.533
12	GRB 200826B	26.08.2020 22:09:42	162.060	10.246	47.962	+0.033	−0.058	+5.468
13	GRB 200829A	29.08.2020 13:59:34	161.190	10.595	79.895	+0.018	−0.022	+2.387
14	GRB 200903E	03.09.2020 02:34:27	160.215	10.958	45.473	+0.190	−0.215	+24.255
15	GRB 201103B	03.11.2020 18:06:45	186.951	−1.159	143.468	+0.118	−0.153	+16.233
16	GRB 201218A	18.12.2020 04:14:15	217.845	−13.777	80.232	+0.030	−0.027	+3.460
17	GRB 210112A	12.01.2021 01:37:03	237.877	−19.880	55.888	+0.100	−0.189	+17.334
18	GRB 210121A	21.01.2021 18:41:48	246.521	−21.785	98.408	+0.031	−0.111	+8.501
19	GRB 210619B	19.06.2021 23:59:25	313.312	−17.792	51.967	+0.024	−0.041	+3.899
20	GRB 210812A	12.08.2021 16:47:01	326.733	−14.601	100.396	+0.104	−0.098	+12.142
21	GRB 210927B	27.09.2021 23:54:45	2.101	−1.674	94.135	+0.034	−0.079	+6.774
22	GRB 211019A	19.10.2021 05:59:31	27.190	10.927	89.034	+0.021	−0.022	+2.605
23	GRB 211022A	22.10.2021 00:47:28	30.161	12.392	125.005	+0.096	−0.214	+18.655
24	GRB 211120A	20.11.2021 23:05:21	48.375	20.195	78.700	+0.031	−0.028	+3.559

Table 3
Grouping of gamma-ray bursts detected and localized by MGNS-HEND instruments.

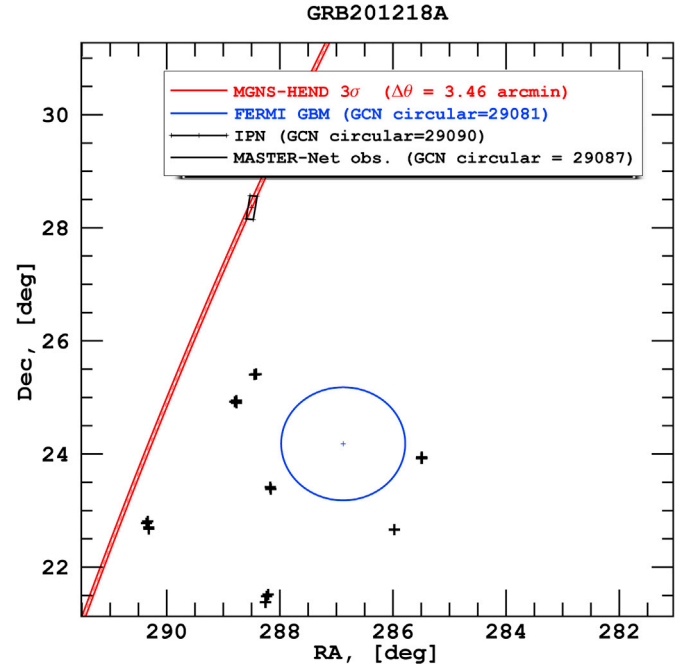| Group	Name	Definition	Quantity
Group 1	Confirmation	A group of gamma-ray bursts in which the localization of MGNS-HEND confirmed the coordinates of the detected optical transient.	8
Group 2	Decreasing of existed error boxes size	A group of gamma-ray bursts for which the error boxes for the GRB source were defined. MGNS-HEND localization confirmed the position and the decrease of existed error boxes size.	11
Group 3	Disapproval of existed error boxes position	A group of gamma-ray bursts for which the error boxes for the GRB source were defined. MGNS-HEND localization disapproved the existed and suggested the new error boxes position.	3
Group 4	Suggestion of new error box	A group of gamma-ray bursts for which no source localization was performed. MGNS-HEND localization is the first localization.	2

Fig. 7. MGNS-HEND triangulation annulus for the bursts GRB201218A from Group 2. The crosses mark the points of observation of optical transients which was not identify with GRB (see GCN circular 29087). The black square corresponds to the error box obtained by the IPN.

Table 3). As it is known, the most precise area for GRB's source localization is provided by the Swift experiment. The error boxes of Swift have not been published for GRB from *Group 2*. For this group, MGNS and HEND localization has significantly improved the size of the available localization error boxes. For 6 GRBs of *Group 2* an optical transient has been searched but no source could be observed. One possible reason being the size of the available error boxes of about a several angular degrees, which cannot be fully covered by large ground-based optical telescopes with highest sensitivity. MGNS and HEND localization could decreases the error box size to a few angular minutes, a significant improvement for the detection of optical transient. An example of the localization of GRB201218A from *Group 2* is shown in Fig. 7.

Group 3 consists of 3 GRBs for which the error boxes published in the GCN have not been confirmed by the localization of MGNS-HEND pair (see Table 3). For these GRBs, it could be proposed a new localization annulus of width of 4–12 angular minutes and significance level of 3σ,

with no crossings with the existing error boxes. An example of the localization of GRB210927B GRBs from Group 3 is shown in Fig. 8.

Group 4 includes the 2 GRBs for which no GCN circulars were issued with localization data (see Table 3). The registration and localization of the GRB is based only on the data of the MGNS-HEND pair of instruments. HEND-MGNS localization, in this case, is unique.

Thus, *Groups 2–4* include 16 of the 24 or about 67% of the GRBs jointly detected by HEND and MGNS. Using data on the localization of these bursts may greatly simplify the task of searching for afterglows,
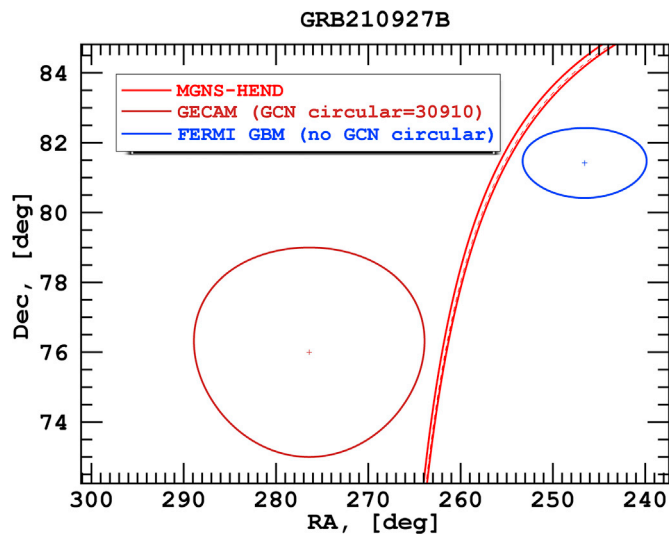
Fig. 8. MGNS-HEND triangulation annulus for the bursts GRB210927B from Group 3. The MGNS-HEND localization annulus has a width of about 6.8 angular minutes at a significance level of 3σ. The radius of error boxes for GECAM and FERMI experiments have values of 3 and 1 angular degree, respectively, at a significance level of 1σ.

since this pair of interplanetary instruments provides a much smaller localization error box than that provided by other near-Earth instruments, and in some cases this localization is unique.

5. Summary

During its first 3.6 years interplanetary cruise to Mercury onboard BepiColombo, MGNS detected 43 confirmed GRBs. For 24 of these GRBs, localization by triangulation in conjunction with the data from HEND were performed and the obtained localization annuli provided an average accuracy of about 13 angular minutes. For 16 GRBs (i.e. *Group 2–4* in Table 3 and Section 4) the localization error box was either significantly improved or a revised error box could be suggested.

The interplanetary position in the solar system of the BepiColombo spacecraft provided a unique opportunity for MGNS to contribute in the IPN program for localization of the GRBs sources. On October 20, 2021, the MGNS instrument joined the Interplanetary Network for the localization of cosmic gamma-ray bursts IPN (Hurley 2021). IPN currently consists of six instruments onboard spacecrafts of Konus-Wind, Mars Odyssey, BepiColombo, Swift, INTEGRAL and AGILE. Two of them are located at an interplanetary distance from the spacecraft to near-to-Earth orbit: MGNS/BepiColombo on a cruise phase to Mercury and HEND/-Mars Odyssey on the Mars orbit. Joining the MGNS to the IPN will lead to more precise GRB localizations with an accuracy of few angular minutes.

During the first 1.5 months of participation of the MGNS instrument in the IPN program, 5 gamma-ray bursts were localized with four of them using the localization annulus obtained from the MGNS-HEND data: GRB 210927B, GRB 211019A, GRB 211022A and GRB 211120A (Kozyrev 2021a-d). Fig. 9 shows an example of an IPN triangulation calculated using the MGNS-HEND data for a GRB211019A. For the GRB 211130A burst, the HEND instrument data were not available, because the source position was below the Mars horizon. Therefore, of all the interplanetary instruments, only data from the MGNS instrument were used to calculate the triangulation (Kozyrev et al., 2021e).

Taking into account the high science performance herewith presented, it was decided that MGNS will operate almost continuously during the cruise and exploration phases of BepiColombo, with exceptions mainly limited to periods of trajectory adjustments. It is expected that the MGNS data will be transmitted to Earth regularly, from daily to once every few days, depending on the distance between the spacecraft
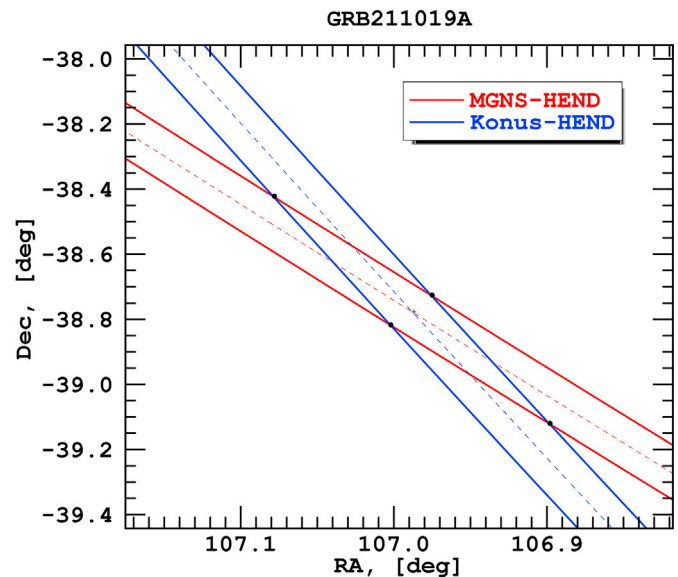

Fig. 9. IPN triangulation (GCN Circular 30993) calculated using MGNS-HEND data for the GRB211019A.

and the Earth. It is expected that the pair of MGNS-HEND instruments will be able to provide precise localization with a detection rate of about 2 gamma-ray bursts per month.

Declaration of competing interest

The authors declare that they have no known competing financial interests or personal relationships that could have appeared to influence the work reported in this paper.

Data availability

The authors do not have permission to share data.

References

Acton, C.H., 1996. Ancillary data services of NASA's Navigation and ancillary information facility. Planet. Space Sci. 44 (No. 1), 65–70. https://doi.org/10.1016/0032-0633(95)00107-7.

Acton, Charles, Bachman, Nathaniel, Semenov, Boris, Wright, Edward, 2017. A look toward the future in the handling of space science mission geometry. Planet. Space Sci. https://doi.org/10.1016/j.pss.2017.02.013.

Benkhoff, J., Murakami, G., Baumjohann, W., et al., 2021. BepiColombo - mission overview and science goals. Space Sci. Rev. 217.

Boynton, W., Feldman, W., Mitrofanov, I., et al., 2003. The Mars Odyssey gamma-ray spectrometer instrument suite. Space Sci. Rev. 110, 37–83.

Chen, C., Xiao, Sh, Xiong, Sh, 2021. Design and test of a portable Gamma-Ray Burst simulator for GECAM. Exp. Astron. 52 (Issue 1–2), 45–58.

Cunningham, V., Cenko, S.B., Vogel, S., 2020. GRB 200219C: VLA Detection. GCN Circular 27298. https://gcn.gsfc.nasa.gov/gcn3/27298.gcn3.

Gehrels, N., Chincarini, G., Giommi, P., Mason, K.O., et al., 2004. The Swift gamma-ray burst mission. Astrophys. J. 611 (2), 1005–1020.

Gendre, B., Corsi, A., Cutini, S., 2009. The TAROT archive: rising afterglows, GAMMA-RAY BURST: sixth Huntsville Symposium. AIP Conf. Proc. 1133, 175–180.

Hurley, K., Pal'shin, V., Aptekar, R., et al., 2013. The interplanetary network supplement to the fermi GBM catalog of cosmic gamma-ray bursts. ApJS 207 (39).

Hurley, K., Svinkin, D.S., Aptekar, R.L., et al., 2016. The interplanetary network response to LIGO GW150914. The Astrophysical Journal Letters 829 (Issue 1), 5 article id. L12.

Hurley, K., Kozyrev, A.S., Golovin, D.V., et al., 2021. BepiColombo MGNS Joins the IPN, BepiColombo MGNS Joins the IPN, GCN Circular, 30949. https://gcn.gsfc.nasa.gov/gcn3/30949.gcn3.

Kouveliotou, C., Meegan, C.A., Fishman, G.J., et al., 1993. Identification of two classes of gamma-ray bursts. ApJL 413, L101.

Kozyrev, A., Mitrofanov, I., Benkhoff, J., et al., 2016 a. Next generation of scintillation detector based on cerium bromide crystal for space application in the gamma-ray spectrometer of the Mercurian Gamma-ray and Neutron Spectrometer. Instrum. Exp. Tech. 59 (No. 4), 569–577.

Kozyrev, A., Mitrofanov, I., Owens, A., et al., 2016 b. A comparative study of $LaBr_3(Ce3+)$ and $CeBr_3$ based gamma-ray spectrometers for planetary remote sensing applications. Rev. Sci. Instrum. 87, 8.

Kozyrev, A.S., Golovin, D.V., Litvak, M.L., et al., 2021a. IPN Triangulation of GRB 210927B. GCN Circular, 30956. https://gcn.gsfc.nasa.gov/gcn3/30956.gcn3.

Kozyrev, A.S., Golovin, D.V., Litvak, M.L., et al., 2021b. IPN Triangulation of GRB 211019A. GCN Circular, 30993. https://gcn.gsfc.nasa.gov/gcn3/30993.gcn3.

Kozyrev, A.S., Golovin, D.V., Litvak, M.L., et al., 2021c. IPN Triangulation of GRB 211022A, GCN Circular 31024. https://gcn.gsfc.nasa.gov/gcn3/31024.gcn3.

Kozyrev, A.S., Golovin, D.V., Litvak, M.L., et al., 2021d. IPN triangulation of GRB 211120A. GCN Circular 31129. https://gcn.gsfc.nasa.gov/gcn3/31129.gcn3.

Kozyrev, A.S., Golovin, D.V., Litvak, M.L., et al., 2021e. IPN Triangulation of GRB 211130A, GCN Circular 31161. https://gcn.gsfc.nasa.gov/gcn3/31161.gcn3.

Lampton, M., Margon, B., Bowyer, S., 1976. Parameter estimation in X-ray astronomy. Astrophys. J. 208, 177–190.

Livshits, M.A., Zimovets, I.V., Golovin, D.V., et al., 2017. Catalog of hard X-ray solar flares detected with Mars Odyssey/HEND from the Mars orbit in 2001-2016. Astron. Rep. 61 (9), 791–804.

Mitrofanov, I.G., Litvak, M.L., Kozyrev, A.S., et al., 2003. Search for water in Martian soil using global neutron Mapping by the Russian HEND instrument onboard the US 2001 Mars Odyssey spacecraft. Astron. Vestn. 37 (5), 400–412. Sol. Syst. Res. (Engl. Transl.), 2003, vol. 37, no. 5, p. 366.

Mitrofanov, I.G., et al., 2010. The Mercury gamma and neutron spectrometer (MGNS) onboard the planetary orbiter of the BepiColombo mission. Planet. Space Sci. 58, 116–124.

Mitrofanov I. G., Kozyrev A. S., Lisov, D. I., et al., The Mercury gamma-ray and neutron spectrometer (MGNS) onboard the Mercury planetary orbiter of the BepiColombo mission: design updates and first measurements in space, Space Sci. Rev., Volume 217, Issue 5, article id.67 (2021).

Paciesas, W., Meegan, C., von Kienlin, A., et al., 2012. The fermi GBM gamma-ray burst catalog: the first two years. The Astrophysical Journal Supplement 199 (Issue 1), 12 article id. 18.

Pal'shin, V.D., Hurley, K., Svinkin, D.S., 2013. Interplanetary network localizations of Konus short gamma-ray bursts. The Astrophysical Journal Supplement 207 (Issue 2), 14 article id. 38.

Reva, I., Pozanenko, A., Krugov, M., et al., 2020. GRB 200219C: Mondy and TSHAO optical observations. GCN Circular 31024. https://gcn.gsfc.nasa.gov/gcn3/27162.gcn3.

Sanna, A., Burderi, L., Di Salvo, T., et al., 2020. Timing techniques applied to distributed modular high-energy astronomy: the H.E.R.M.E.S. project. Proc. SPIE 11444, 114444X 19.

Tavani, M., Barbiellini, G., Argan, A., et al., 2008. The AGILE space mission. Nucl. Instrum. Methods Phys. Res., Sect. A 588 (Issue 1–2), 52–62.

Winkler, C., Courvoisier, T.J.-L., Di Cocco, G., et al., 2003. The INTEGRAL mission. Astron. Astrophys. 411, L1–L6.

Xu, D., Liu, X., Zhu, Z.P., et al., 2020. GRB 200219C: Nanshan/NEXT optical upper limit and possible host galaxy from PanSTARRS. GCN Circular 27161. https://gcn.gsfc.nasa.gov/gcn3/27161.gcn3.

Zhang, B., Fan, Y.Z., Dyks, J., 2006. Physical processes shaping gamma-ray burst X-ray afterglow light curves: theoretical implications from the Swift X-ray telescope observations. Astrophys. J. 642 (1), 354–370.